Available online at www.sciencedirect.com
ScienceDirect
Journal of Colloid and Interface Science 305 (2007) 275–279
JOURNAL OF Colloid and Interface Science
www.elsevier.com/locate/jcis

Mesoporous silica reinforced by silica nanoparticles to enhance mechanical performance

Jen-Tsung Luo [a,*], Hua-Chiang Wen [a], Yu-Ming Chang [a], Wen-Fa Wu [b], Chang-Pin Chou [a]

[a] *Department of Mechanical Engineering, National Chiao Tung University, Hsinchu, Taiwan*
[b] *National Nano Device Laboratories, Hsinchu, Taiwan*

Received 21 June 2006; accepted 24 September 2006

Available online 23 October 2006

Abstract

Silica nanoparticle/mesoporous silica composite films were prepared by direct mixing with mechanical stirring and thermal imidization. The structural morphology was elucidated by scanning electron microscopy and the surface of the film was imaged by atomic force microscopy. The functional groups and desorption process of the films were elucidated by Fourier transform infrared spectroscopy and thermal desorption spectroscopy. The mechanical properties were investigated using a nanoindenter system. The gel matrix and the filler are very compatible because they have similar molecular content. The composite films had a higher mechanical strength than pure porous silica film. Their strength is related to the silica nanoparticle content. The interfacial compatibility, dispersion effect, and interfacial strength also affect the mechanical strength of composite films.

Keywords: Porous silica; Nanoparticle; Composite material; Mechanical properties

1. Introduction

Porous silica materials have attracted much attention in recent years owing to their low density, high chemical stability, low dielectric constant, and high thermal resistance [1,2]. Functional porous silica gels, such as mesoporous silica and bimodal porous silica, have been developed and studied [3,4]. However, the introduction of porosity degrades the mechanical properties of porous silica film, including its strength and elastic modulus, and limits the range of its applications. The potential use of inorganic materials as fillers in porous silica composites in industrial and technological applications has been noted. In this investigation, a reinforcing filler, nanoscale silica particles, is employed to increase the mechanical strength of mesoporous silica material. Ceramic-like particles, such as silica nanoparticles, are used as inorganic fillers in the preparation of composite materials by the sol–gel process [5–7] or by in situ technique [8]. The silica reinforcement and porous silica matrix comprise mainly tetraethyl orthosilicate (TEOS), with which they have similar physical and chemical characteristics; they have a large inorganic surface area to have the best balance of the mechanical strength [9]. The silica filler also has some advantages, such as surface modification and thermal stability. The filler and the matrix were mixed by co-polymerization to yield composites with good dispersion. Some works have also reported the method of dispersion and demonstrated an approach to preventing the aggregation of silica nanoparticles by modifying silica surfaces. These approaches have many applications when their large-scale manufacturing processes are scaled down to the nanoscale. Porous silica films are manufactured by the high-temperature hydrolysis of TEOS in a furnace. Therefore, during thermal processes, some silanol and siloxane groups are also formed on the surface. The silanol-dominant surface is chemically modified to yield hydrophobic characteristics and thus produce a hydrophobic surface. The hydrophobic films had not only a reduced silanol group density but also an increased specific surface area.

The mechanical properties of the composite will be extensively improved as the diameter of the filler falls to the nanoscale, increasing the surface area/volume ratio. Silica

* Corresponding author. Fax: +886 3 5733409.
E-mail address: oam.me90g@nctu.edu.tw (J.-T. Luo).

0021-9797/$ – see front matter
doi:10.1016/j.jcis.2006.09.066

nanoparticles with a larger surface area/volume ratio have a higher reinforcing efficiency, even at low filler concentration. The reinforcing effect is also typically associated with the degree of particle irregularity, spherical geometry, and surface roughness. The use of silica nanoparticles in mesoporous silica films normally is an effective way to improve the overall mechanical properties over the prior molecular composition.

2. Experimental

The silica particles were supplied by the Desun Company. They contained more than 98% SiO_2 and had an average diameter of around 100 nm. The silica particles was first mixed in ethanol solution and stirred at 300 rpm for 1 h to facilitate adequate dispersion. The mesoporous silica sol–gel was prepared by adding TEOS to ethanol with HCl catalyst. Tween 80 (polyoxyethylene(20) sorbitan monooleate) serves as a molecular template. Ethanol and deionized water are the solvents. The gel mixture ratio of TEOS:ethanol:HCl:H_2O:Tween 80 is 12:21:1.2:3.4:9.6 (by weight). The gel solution was mechanically stirred at room temperature. Different amounts of solvent–silica particle mixtures were added to the mesoporous silica–gel. They were ultrasonicated with water reflux for 3 h. After the homogeneous solutions had been obtained, the solutions were coated on silicon or glass substrates. Then they were soft-baked at 106 °C for 1 h and cured at 400 °C for 30 min. The mesoporous structure was formed by burning off a molecular template (Tween 80) to form air pores. Hexamethyldisilazane (HMDS)–toluene solution was adopted to replace the unconverted surface silanol groups as trimethylsilane groups.

The surface modified films were then baked at 105 °C in ambient air for 3 min. SEM was utilized to characterize the microstructures and interface image of the film. The roughness and the surface morphology were elucidated by AFM. The surface functional groups were verified by FTIR spectroscopy. The outgassing behavior and chemical desorption was examined by making TDS measurements. The refractive indices of the composite films were tested using an optical instrument, an N&K analyzer. The mechanical characteristics, such as the Young's modulus and hardness, were estimated using a nanoindenter system, which could apply a force to an area on the micro to nanoscale. A sharp diamond indenter applied a small force to the tested samples and the force was recorded as a function of the indentation depth. The Young's modulus and hardness are calculated from the indentation curve [10–12].

3. Results and discussion

Fig. 1 shows the AFM image made to elucidate the film's surface morphology. The maximum height is approximately 91 nm and some silica particles are uniformly distributed on the surface. The mean diameter of the particle is about 100 nm; however, some aggregate to form silica grains that are larger than the original silica particles (100 nm). The content of the filler influences the distribution of the particles [13]. If the content of the silica particle exceeds a threshold content, the aggregation of silica grain will form. The sol–gel composite solution with high silica nanoparticle content tends to produce aggregates, which will result in the residual stress in the interface between the filler and the matrix. Therefore, if a uniform surface structure is intended to be obtained, then the silica nanoparticle content should not exceed that at the initiation of aggregate.

Fig. 2a shows the fracture section of SEM image. Distinguishing silica particles from the surrounding matrix is difficult. The fracture section of the composite sample was relatively rough. A series of sheets indicated that a crack propagated some obstacles during the failure process, which can be explained by the deflection of cracks and the continual propagation of cracks on two slightly different fracture planes. A large quantity of silica particles may also result in a high degree of roughness. Figs. 2b and 2c show the chemically etched and unetched surface images of the composite films, where 3 wt% silica particles are dispersed in the matrix. Some of the silica particles are well dispersed, while some formed large aggregates, dispersed locally in the surface. Reportedly, increasing the number of hydrophobic groups on the surface of silica nanoparticle prevents the aggregation of silica particles [14]. The aggregation

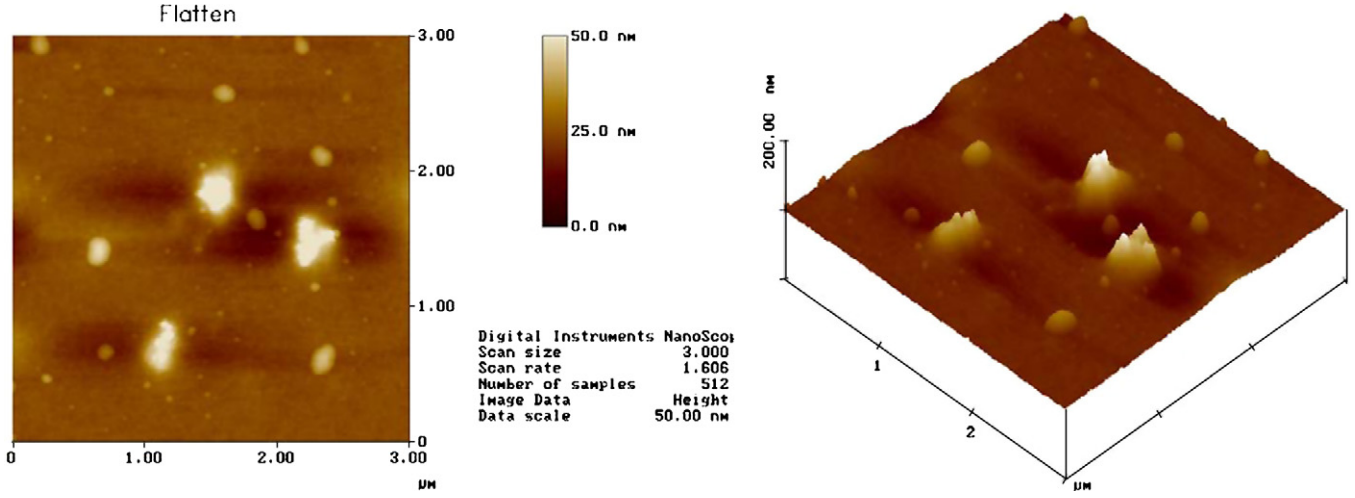

Fig. 1. AFM image of mesoporous silica composite film.

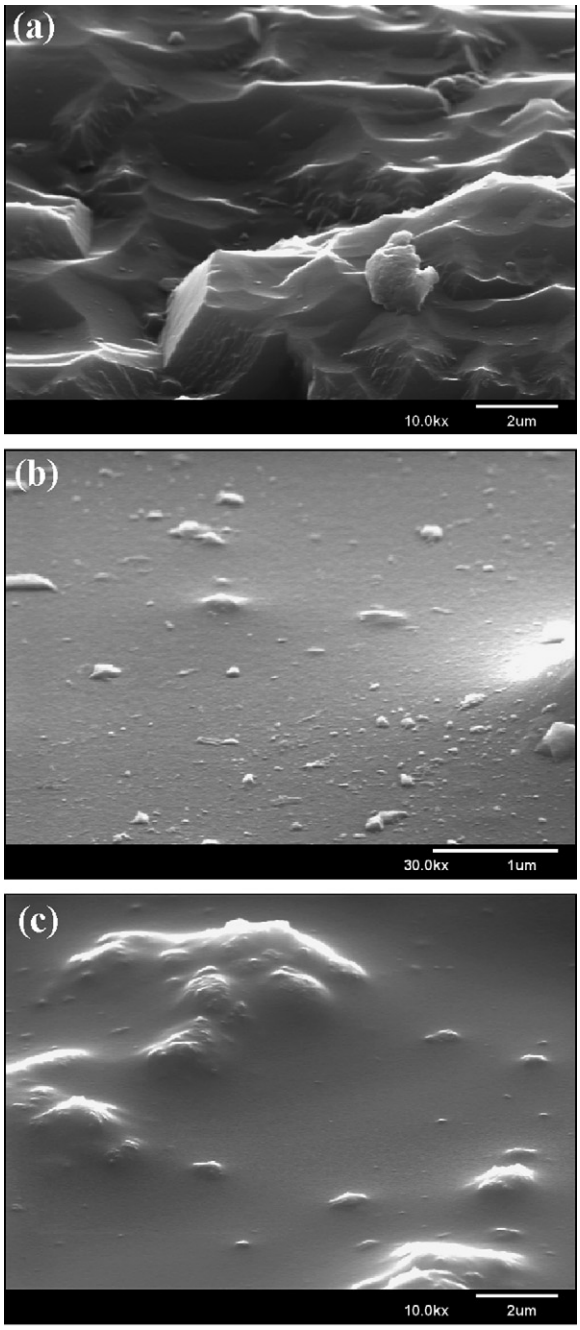

Fig. 2. SEM image of mesoporous silica composite films: (a) fracture image, (b) chemically etched surface image, and (c) unetched surface image.

of the filler resulted in the poor mechanical properties of the composite material. The mechanical properties of the modified nanocomposites are also related to the interaction across the interface. The other determinant of the agglomerates is the screwing speed. A high screw speed can break up agglomerates and create a new interface.

Fig. 3 plots the Young's modulus and hardness of the coating films as functions of the silica particle content. When no silica filler is added, the surface of the film is soft, with a hardness of about 0.6 GPa, and the Young's modulus is about 6 GPa. When the filler content is around 5%, the hardness and Young's modulus increase to about 0.92 and 16.6 GPa, respectively. The hardness and Young's modulus increased gradually with the silica particle content. The molecular steric structure of sp^3 and the volume fraction of the pore influence the mechanical strength of a pure porous silica film. The hardness of the film increases with the sp^3 content. However, increasing the volume fraction of the pores degraded the mechanical properties. The hardness and Young's modulus of composite materials increased with the weight fraction of the silica particles, mainly because of the dispersion effect and the interfacial strength. The effective loading transfer from the matrix to the filler is predicted when the silica particles were dispersed effectively and strongly bonded with the matrix molecules. The porosities of the films, presented in Table 1, can be determined from the refractive index, according to the Lorentz–Lorenz relationship [15]. The addition of the silica particles reduced the porosity of the film and increased the surrounding density of the film. Hence, the hardness and Young's modulus were increased. Fig. 4 plots the penetration depth and the loading curve of the composite films. The coordinate h_{fin} is the position where the indenter was detached from the specimen surface. The coordinate $h_{\max}$ is the position where the penetration depth of the indenter reached its maximum value. The maximum loading is around 600 mN. Bolshakov and Pharr reported that all materials with an $h_{\text{fin}}/h_{\max}$ ratio of under 0.7 exhibit sin-in, while those with an $h_{\text{fin}}/h_{\max}$ ratio of over 0.7 show pile-up, because of the difference between the stress concentrations induced in the material during nanoindentation [16,17]. A higher silica filler content corresponds to a higher loading force.

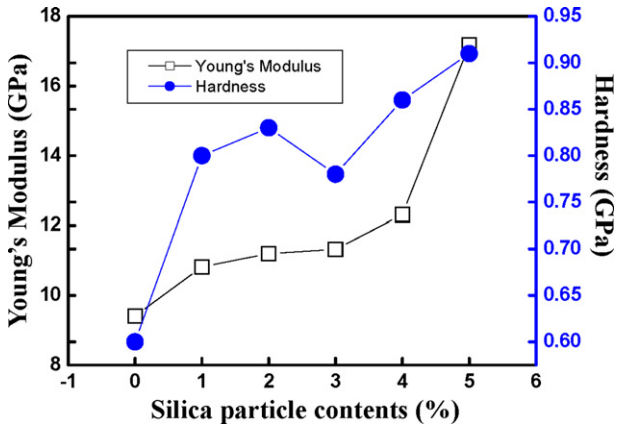

Fig. 3. Effect of silica nanoparticle content on the hardness and Young's modulus of composite films.

Table 1
Refractive index and porosity of composite films with different silica particle contents

Samples	Refractive index (n)	Porosity (%)
As deposited	1.22	48
1%	1.25	38
3%	1.27	36
5%	1.28	35

FTIR was utilized to study the chemical interactions and bonding structures. Fig. 5 shows the FTIR spectra at wavenum-

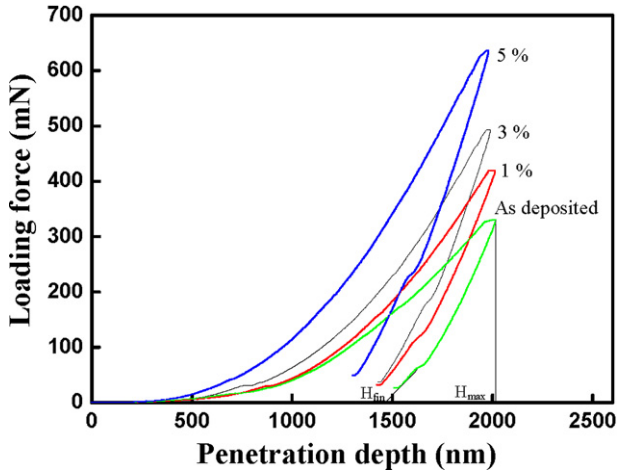

Fig. 4. Loading force vs penetration depth of composite films with different silica particles content.

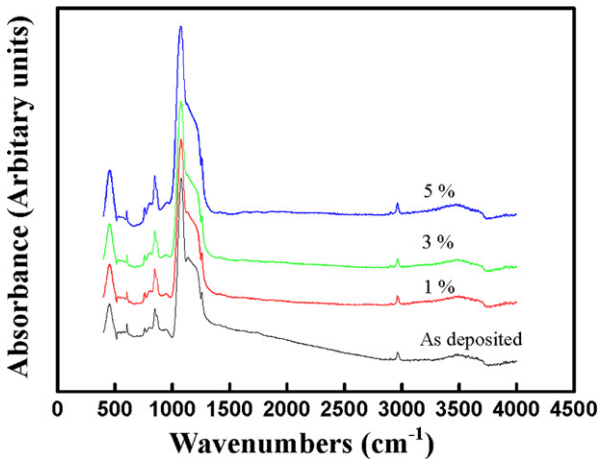

Fig. 5. FTIR spectra of composite films with different silica particle content.

bers 400–4000 cm^{-1}. The silica nanoparticles were isolated from the ethanol emulsion by the evaporation of the solvent. The main components at around 1060 to 1260 constituted the skeletal SiO_2 network. The asymmetric stretching mode of the Si–O groups is at 1072 cm^{-1}. Two peaks at 1290 and 1160 cm^{-1} are probably related to the splitting mode into a transverse optical/longitudinal optical (TO–LO) pair in the time domain for low-symmetry phonons that were excited from different crystallographic faces [18,19]. The appearance of the TO–LO shoulder is related to the porosity of the samples. The shape of this band depends on the molecular structure of the silica network and evolves appreciably upon thermal condensation. The peak at 798 cm^{-1} is attributable to the symmetric Si–O–Si stretching vibration and the bending mode, which is affected by the equilibrium bond angle, is present at 455 cm^{-1}. The trimethylsilyl groups in the surface were revealed by the presence of the two absorption peaks at 1255 and 2960 cm^{-1}. The silanol group (Si–OH) peak is at 3400 cm^{-1}, indicating incomplete condensation in the presence of conspicuous hydroxyl groups on the surface of the mesoporous silica films. The number of surface silanol groups can be reduced by plasma or hydrophobic modification. The presence of silica particles in the system does not inhibit nanopore separation but accelerates gel formation. The mechanical properties of the composite film are improved by interfacial compatibility, which is probably strengthened by the hydrogen bonds, copolymerization, or the chain reaction of Si–C–Si (1050 cm^{-1}).

The outgassing behavior of O_2, CH_4, H_2O, and CO_2 was investigated using a TDS system. Fig. 6a shows the thermal desorption traces of O_2 ($m/e = 32$) at a heating rate of 20 °C/min. In the peak spectrum, maximum desorption (T_{max}) is at 300 °C, and a little oxygen was detected at over 500 °C. The peak at 300 °C is the desorption of chemical adsorption and surface oxygen. The T_{max} is related to the desorption temperature of the activation energy. The increase in the desorption temperature reveals an increase in the depth of penetration of oxygen molecules, whose diffusion behavior is like that of a free gas [20]. According to the literature, the penetration depth of O_2 exceeds several nanometers [21]. In this work, O_2 is located in the upper atomic layer of the surface. Fig. 6b shows the CO_2 ($m/e = 44$) desorption peak. Carbon monoxide (CO) molecules were adsorbed at room temperature and oxidized to CO_2. CO_2 decomposed at about 400 °C. The CO_2 molecule is bound through the carbon atom, which might be the residual organic solvent or the oxidation of CH_x groups, which are attached to the surface plane. The CO_2 molecules started to occupy more coordinated hollow/bridge sites. From the desorption curve, the as-deposited sample occupied the largest area while the 5% sample occupied the least area. Fig. 6c shows the outgassing behavior of H_2O. Some scattered data were obtained, especially at temperatures under 200 °C. The desorption intensity increased with the high silica–particle content. Below 200 °C, the desorption behavior is physical desorption. The amount of H_2O desorbed reflects the water affinity of the films. The water is desorbed by the porous structure. If the porous silica surface loses some of its hydrophobicity, then a large amount of water will be adsorbed in the mesopores by capillary condensation. The amount of desorbed H_2O depends on temperature and the total volume of the pores. Fig. 6d shows the decomposition behavior of methyl, which is a nonpolar group with hydrophobic properties on the surface of the film. The organic groups on the surface may come from the residual solvent and the surface modification agent. The desorption curves increased linearly with temperature.

4. Conclusions

In this study, an easy route for synthesizing a strong silica/mesoporous silica composite film is achieved by combining the sol–gel and ultrasonic methods. FTIR measurements reveal that the matrix and reinforcement are chemically and physically compatible with each other. Silica nanoparticles were proven to provide greater strength and stiffness than mesoporous silica material. Mechanical tests indicated that the loading force was transferred from the matrix to the filler, with better mechanical results. The strength was closely related to the weight fraction of silica particles. It is also suggested that the increased strength is due to the increase of density of porous silica composite films.

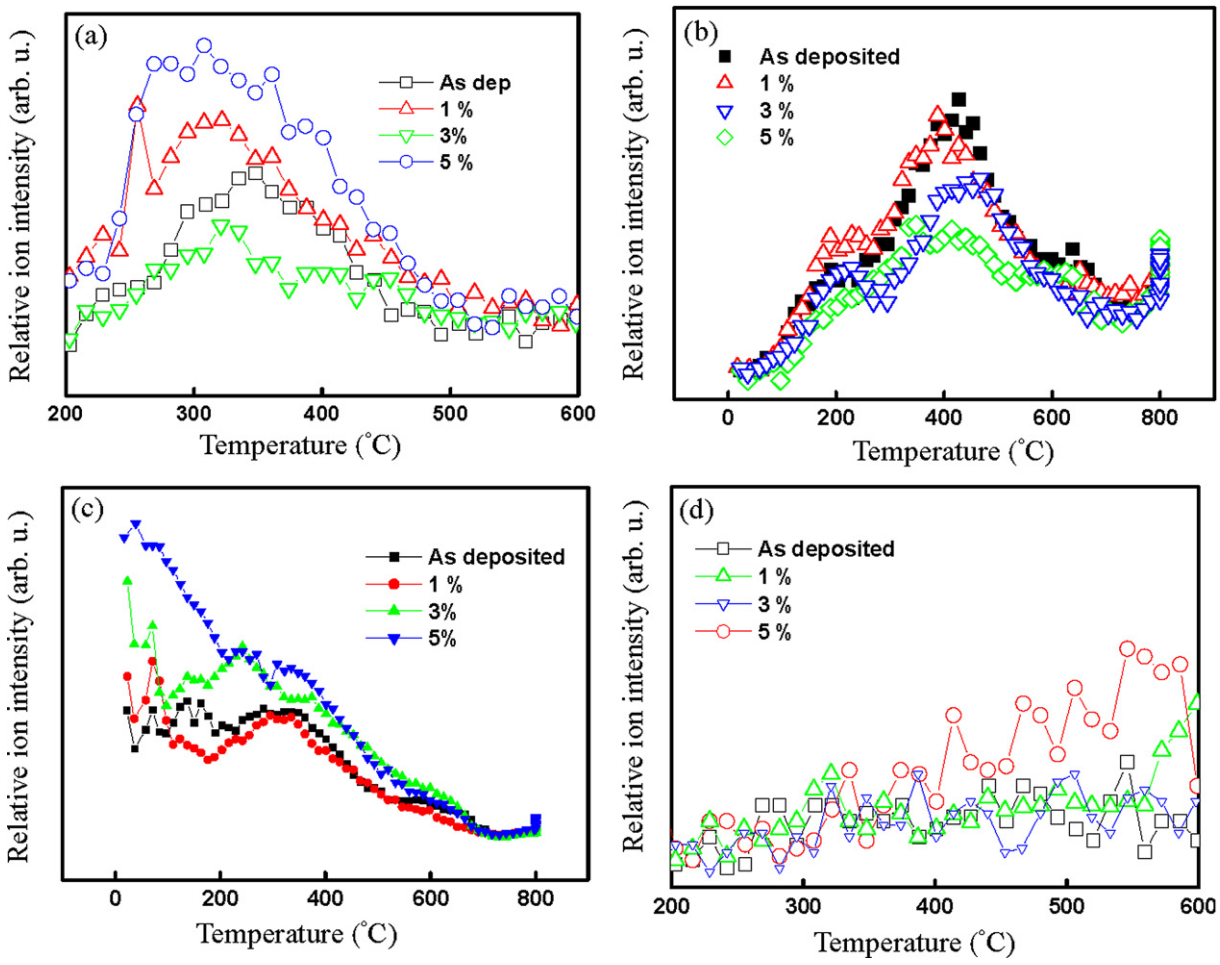

Fig. 6. Production of thermal desorption elements as a function of temperature with different silica nanoparticle content: (a) O_2 ($m/e = 32$), (b) CO_2 ($m/e = 44$), (c) H_2O ($m/e = 18$), and (d) CH_4 ($m/e = 16$).

References

[1] C.T. Kresge, M.E. Leonowicz, W.J. Roth, Nature 359 (1992) 710.
[2] J.S. Beck, J.C. Vartuli, J. Am. Chem. Soc. 114 (1992) 10,834.
[3] Y. Fukushima, S. Inagaki, Mater. Sci. Eng. A 217 (1996) 116.
[4] Y. Zhao, J. Zou, W. Shi, L. Tang, Micropor. Mesopor. Mater. 92 (1–3) (2006) 251.
[5] H. Peng, J. Tang, L. Yang, J. Pang, Z. Yang, Y. Lu, J. Am. Chem. Soc. 128 (16) (2006) 5304.
[6] Y.Y. Yu, C.Y. Chen, W.C. Chen, Polymer 44 (2003) 593.
[7] W.C. Chen, L.H. Lee, Chem. Mater. 13 (2000) 3320.
[8] K. Haraguchi, Y. Usami, K. Yamamura, S. Matsumoto, Polymer 39 (25) (1998) 6243.
[9] Y. Nakamura, M. Yamaguchi, M. Okubo, T. Matsumoto, J. Appl. Polym. Sci. 45 (1992) 1281.
[10] R. Jayaganthan, K. Mohankumar, A.A. Tay, J. Appl. Phys. 4 (2) (2005) 197.
[11] G.W. Pharr, W.C. Oliver, F. Brotzen, J. Mater. Res. 7 (3) (1992) 613.
[12] W.C. Oliver, G.M. Pharr, J. Mater. Res. 7 (6) (1992) 1564.
[13] S. Gopi, N. Alex, W. Darsh, J. Colloid Interface Sci. 272 (2004) 167.
[14] H. Takeuchi, S. Nagira, H. Yamamoto, Y. Kawashima, Powder Technol. 141 (2004) 187.
[15] M. Born, E. Wolf, Principles of Optics, Pergamon, New York, 1983, p. 87.
[16] R. Smith, D. Christopher, S.D. Kenny, A. Richter, B. Wolf, Phys. Rev. B 67 (2003) 245405.
[17] A. Bolshakov, G.M. Pharr, J. Mater. Res. 13 (4) (1998) 1049.
[18] O.V. Misochko, M.V. Lebedev, T. Dekorsy, J. Phys. Condens. Matter. 17 (2005) 3015.
[19] F.L. Galeener, G. Lucovsky, Phys. Rev. Lett. 37 (1976) 1474.
[20] S. Satoh, I. Matsuyama, K. Susa, J. Non-Cryst. Solids 190 (1995) 206.
[21] J.J. Perez-Bueno, R. Ramırez-Bon, Y.V. Vorobiev, F. Espinoza-Beltranb, Thin Solid Films 379 (2000) 57.